

Characterization and performance of the ASIC (CITIROC) front-end of the ASTRI camera

D. Impiombato^{a,*}, S. Giarrusso^a, T. Mineo^a, O. Catalano^a, C. Gargano^a, G. La Rosa^a, F. Russo^a, G. Sottile^a, S. Billotta^b, G. Bonanno^b, S. Garozzo^b, A. Grillo^b, D. Marano^b, G. Romeo^b

^a*INAF, Istituto di Astrofisica Spaziale e Fisica cosmica di Palermo, via U. La Malfa 153, I-90146 Palermo, Italy*

^b*INAF, Osservatorio Astrofisico di Catania, via S. Sofia 78, I-95123 Catania, Italy*

Abstract

The Cherenkov Imaging Telescope Integrated Read Out Chip, CITIROC, is a chip adopted as the front-end of the camera at the focal plane of the imaging Cherenkov ASTRI dual-mirror small size telescope (ASTRI SST-2M) prototype. This paper presents the results of the measurements performed to characterize CITIROC tailored for the ASTRI SST-2M focal plane requirements. In particular, we investigated the trigger linearity and efficiency, as a function of the pulse amplitude. Moreover, we tested its response by performing a set of measurements using a silicon photomultiplier (SiPM) in dark conditions and under light pulse illumination. The CITIROC output signal is found to vary linearly as a function of the input pulse amplitude. Our results show that it is suitable for the ASTRI SST-2M camera.

Keywords:

Front-end: ASIC for SiPM, ASTRI, CITIROC

*Corresponding author. Tel.: +39 0916809468; fax: +39 0916882258

Email addresses: Domenico.Impiombato@iasf-palermo.inaf.it (D. Impiombato), Giarrusso@iasf-palermo.inaf.it (S. Giarrusso), Mineo@iasf-palermo.inaf.it (T. Mineo), Catalano@iasf-palermo.inaf.it (O. Catalano)

1. Introduction

The global effort in designing and constructing the Cherenkov Telescope Array (CTA), which will have a ten times higher sensitivity than currently operating Cherenkov telescopes [1, 2], is justified by the need of increasing the sensitivity in the very-high energy (VHE) sky observations. Among CTA scientific goals, some pertain to the VHE regime, such as the understanding of the origin of cosmic rays, the nature of particle acceleration in shock regions observed in supernova remnants and in black hole jets, and to unveil the enigmatic nature of dark matter.

The Italian contribution to the CTA Project is mainly represented by the ASTRI (Astrofisica con Specchi a Tecnologia Replicante Italiana) program [3], a flagship project currently financed by the Italian Ministry of Education, University and Research (MIUR) and led by the Italian National Institute for Astrophysics (INAF). Its primary target is to develop an end-to-end prototype of the small-size class of telescopes (SST) devoted to the study of the highest gamma-ray energy range (from a few TeV up to 100 TeV and beyond). The prototype, named ASTRI SST-2M, is characterized by innovative technological solutions adopted for the first time in the design of Cherenkov telescopes: the optical system is arranged in a dual-mirror (2M) configuration [4, 5], and the camera at the focal plane is composed of a matrix of multi-pixel silicon photo-multipliers [6–10].

The telescope is based on a dual-mirror Schwarzschild-Couder design that allows for a compact optical configuration with the ratio of the lens's focal length to the diameter of the entrance pupil equal to 0.5. The focal length is 2.15 m and the full field of view (FoV) is 9.6° .

Using SiPMs instead of the traditional photo-multiplier tubes (PMTs) offers advantages in terms of an excellent single photon resolution, high photon detection efficiency (PDE), low bias voltage (of the order of 70-73V), no damage due to ambient light. The drawbacks in the version of the sensors used for ASTRI-SST 2M are: high dark rate ($> 1\text{MHz}$) optical cross talk ($> 20\%$) and a gain

which is strongly dependent on temperature. Such drawbacks, however, do not prevent SiPMs from being used as detectors at the focal plane of a Cherenkov telescope. In fact, the dark count rate (DCR)($\sim 1\text{MHz}$) is well below that of the night sky background (NSB)($\sim 40\text{MHz}$) and the gain can be kept stable with adequate feedback control of temperature and over-voltage settings while optical cross talk is lower than the intrinsic statistic fluctuation of the number of Cherenkov photons in air showers.

The very short (a few tens of ns) duration of the Cherenkov light flashes associated with showers, requires a front-end electronics (FEE) able to provide auto-trigger capability and fast camera pixel read out. The earlier FEE proposed for ASTRI was based on the extended analogue silicon photo-multiplier integrated read out chip (EASIROC) [11, 12], a commercial application-specific integrated circuit (ASIC) for SiPM read out. Its characterization, performed with detailed measurements [13, 14], proved that EASIROC fulfills the ASTRI requirements for the trigger time walk (5.5 ns), jitter (below 0.3 ns), electronic noise levels and electronic cross talk between channels. Moreover, EASIROC is capable of providing auto-triggering as required by the very short duration of the air shower events. When a pixel detects a signal above the set threshold, a trigger is generated and sent to a Field Programmable Gate Array (FPGA) that produces and sends back a hold signal (HOLD-*B*) to all 32 channels to stop the acquisition and to start the output read out. At the hold time, directly set by the user using a track-and-hold cell, the chip saves the amplitudes of the preamplified and the shaped signal. Unfortunately, the ASIC shows in the high-gain (HG) electronics chain a drift of 20-30ns in the peaking time of the shaped signal that depends on the amount of injected charge. In addition to that, the signal in a shower has an intrinsic duration of the order of 10-30ns and the involved pixels are fired at different times. When the camera trigger is set, all pixel signals are sampled at the same time and then the two effects will produce a degradation of energy resolution of the event, because the signals are read at different points of the shaping function.

To solve this problem, as explained later on, a peak detector circuit has

been implemented in a new version of the EASIROC ASIC, named CITIROC (Cherenkov Imaging Telescope Integrated Read Out Chip), leaving the still suitable parameters unchanged.

In this paper, we present a set of measurements to characterize the new functionalities introduced in CITIROC [15]. We evaluated the optical cross talk and the gain variation as a function of SiPM operating voltage and temperature. In particular, we describe the ASTRI focal plane and the CITIROC device in section 2 and 3, respectively. The laboratory setup is presented in section 4 and the results of the CITIROC characterization are given in section 5. The SiPM performance using CITIROC is presented in section 6 and our conclusions are discussed in section 7.

2. The ASTRI SST-2M camera

The camera at the ASTRI SST-2M focal plane is based on monolithic Hamamatsu SiPMs S11828-3344m¹ with 4×4 squared physical pixels, $3\times 3\text{mm}^2$ each and made up of 3600 elementary diodes of $50\ \mu\text{m}$ pitch, yielding a filling factor of 62%. In order to match the angular resolution of the optical system, the physical pixels are grouped in 2×2 logical pixels ($6.2\times 6.2\text{mm}^2$) with a sky-projected angular size of 0.17° that includes 80% of the optical point spread function (PSF). A complete characterization of the ASTRI SST-2M SiPMs using physical pixels is reported in [16]. Considering the size of the optical area of ASTRI SST-2M, energy range from a few TeV up to 100 TeV and beyond, the requirement for the maximum number of photoelectrons (pe) detected in one pixel is 1000 with a goal of 2000.

For modularity and fast read out of the focal plane, the detector units are organized in an array of 37 photon detection modules (PDM), each with 8×8 logical pixels (see Fig. 1). Two CITIROC ASICs are then necessary to read a single PDM, since each CITIROC chip contains 32 channels (see Fig. 2).

¹<http://www.hamamatsu.com/sp/hpe/HamamatsuNews/HEN111.pdf>

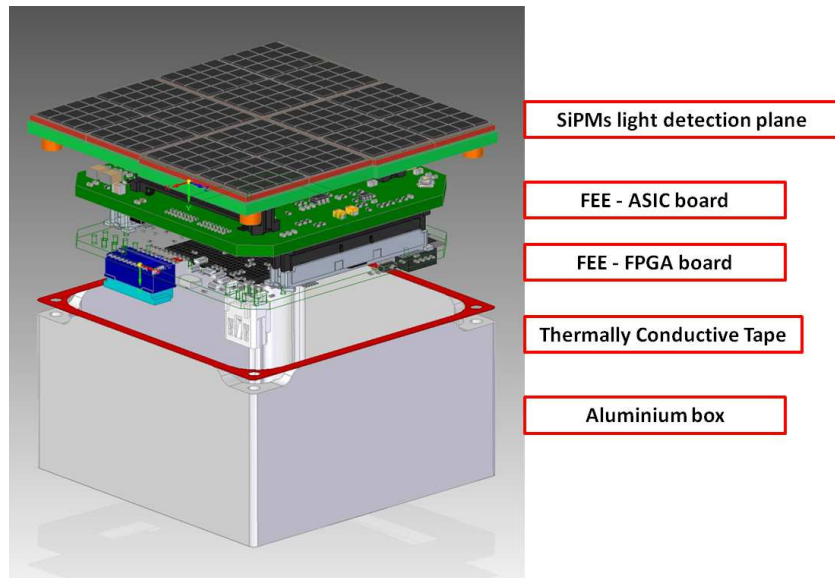


Figure 1: A schematic view of the PDM mechanical assembly.

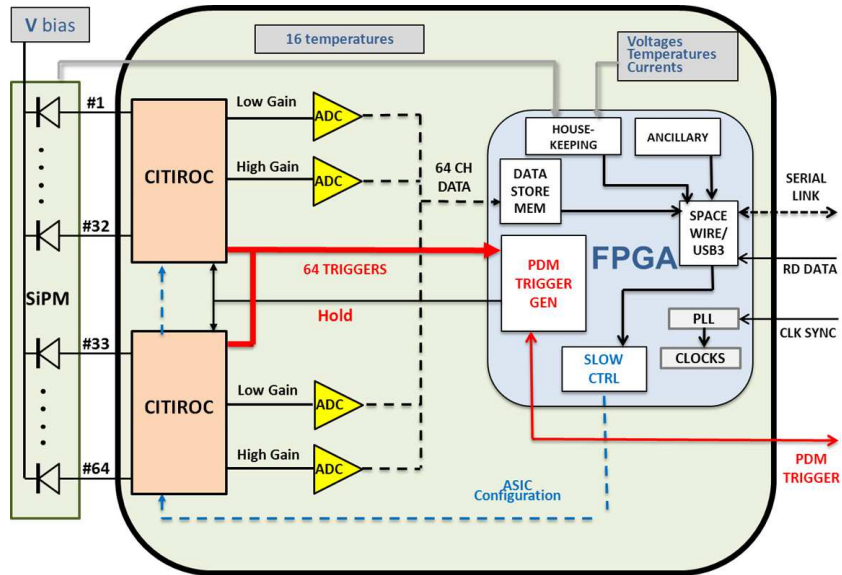


Figure 2: A schematic view of the connections to the ASICs.

The telescope trigger is activated when n contiguous pixels within a PDM present a signal above the discriminator threshold.

The number n of contiguous pixels and the trigger threshold are chosen in order to have a maximum rate of ~ 600 Hz from the whole camera, ensuring a dead time $< 3\%$, according to the CTA requirements. From simulations, we evaluated that 5 contiguous pixels with a discriminator threshold above 4 pe in each pixel gives an average rate lower than requirement.

3. The CITIROC chip

CITIROC, designed by WEEROC², is based on the EASIROC architecture with the addition of custom functions as required by the ASTRI team (see Fig. 3). It is a 32 channel fully analog front-end ASIC designed to read out SiPMs for single photon detection. Its analog core and characteristics are shown in Fig. 4 and listed in Table 1, respectively. The processing of the analog signal takes place in the front-end channels of the device, while the read out is handled at the internal back-end of the ASIC.

Two separate electronics chains allow for high- and low-gain (HG and LG) simultaneous processing of the analog signal.

Each of the two chains is composed (see Fig. 4) of an adjustable preamplifier followed by a tunable shaper (SSH: slow shaper), a track-and-hold circuit (SCA: switched capacitor array) and an active peak detector (PD: peak detector) to capture and hold the maximum value of signal. Fine-tuning of each pixel gain is obtained adjusting the voltage applied to the SiPM through an 8-bit digital-to-analog converter (DAC) ranging from 0 to 4.5 V.

A third chain implements the trigger channel generation using a fast shaper (FSB: bipolar fast shaper) with fixed shaping time of 15 ns, followed by two discriminators. A 10-bit DAC common to all 32 channels, sets the programmable threshold to the discriminators (see Fig. 4). The first of two discriminators, that can also be masked, gives a single output for all channels, while the second one provides a different output for each channel. The topological trigger (see

²<http://www.weeroc.com>

Sect. 2), implemented in the ASTRI SST-2M camera, can be obtained from the second. All CITIROC main parameters can be programmed by downloading a configuration bit-string through a slow-control serial line. The outputs of all the channels can be read out by multiplexing, in parallel, the analog buffers of the HG and LG chains.

An evaluation board has been designed by WEEROC to test the functional characteristics and performance of the ASIC. It allows easy access to the CITIROC outputs and provides many test points to the FPGA³ dedicated lines. It is equipped with two external analog-to-digital converter (ADC) to allow the reading of the analog processed data by the ASIC in digital form.

A Lab-VIEW⁴ software procedure, developed by the LAL (Laboratoire de l'Accélérateur Linéaire) Tests group⁵, has been provided, together with the evaluation board, to command the CITIROC chip and receive the outputs via universal serial bus (USB) connection.



Figure 3: CITIROC chip $4.9 \times 4.6 \text{mm}^2$ (courtesy of WEEROC).

³Altera Corporation - Cyclone FPGA Model EP3C16Q240C8N

⁴<http://www.ni.com/labview/i/>

⁵ <http://www.lal.in2p3.fr/>

Table 1: Main characteristics of the CITIROC chip.

Technology:	Austria-Micro-Systems (AMS) SiGe 0.35 μm
Dimensions :	16.5 mm ² (4.1×4.1mm)
Power Supply :	4.5 V/0 V
Consumption:	2 mW per channel
	95 mW in data transmission mode (all outputs on)
Inputs:	32 voltage inputs with independent SiPM HV adjustments
Outputs:	32 trigger outputs
	1 multiplexed charge output
	1 ASIC trigger output (Trigger OR)
Internal Programmable Features:	32 HV adjustments (one for each channel) (32x8bits)
	Trigger Threshold Adjustment (common for all channels) (10bits)
	Gain tuning (channel by channel)
	32 Trigger Masks
	Channel by channel output enable
Package :	Naked (PEBS) TQFP160

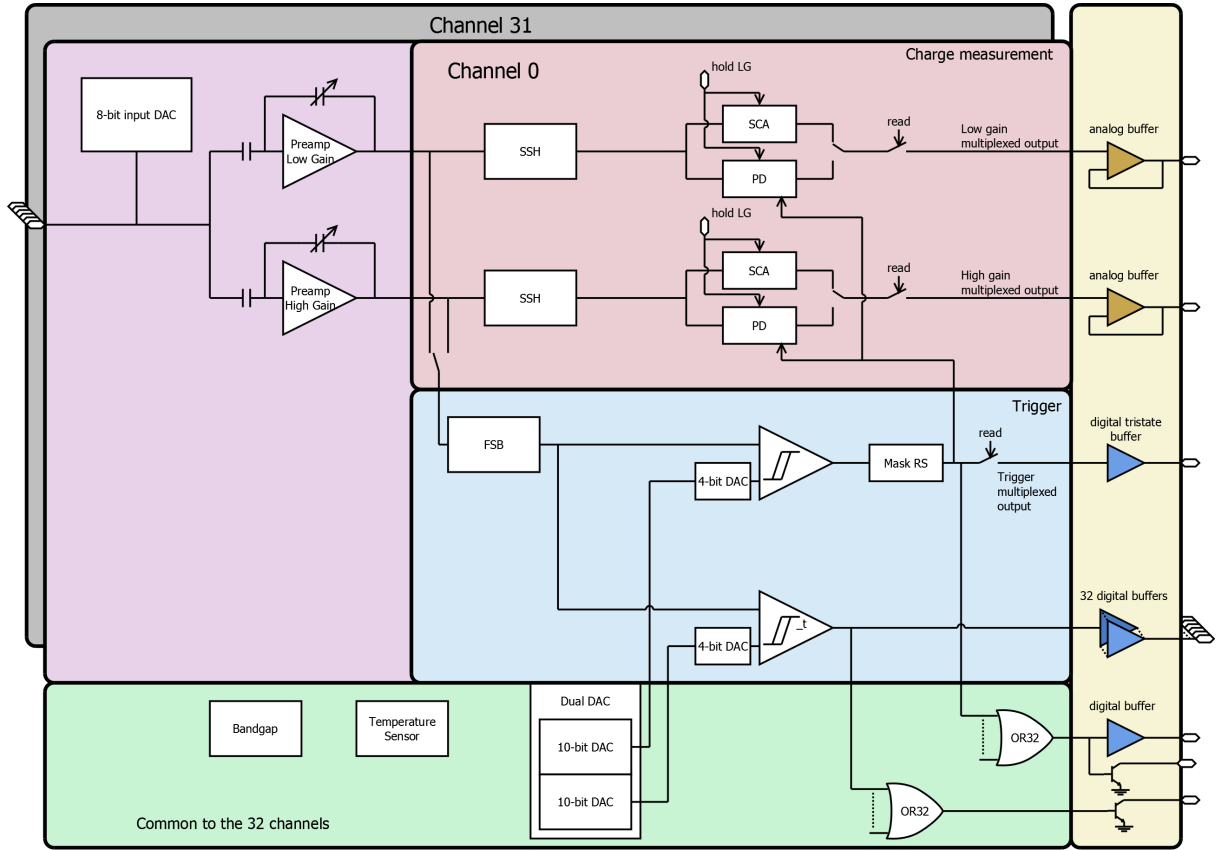


Figure 4: Architecture of the front-end CITIROC (courtesy of WEEROC).

4. Laboratory set-up

We performed two different sets of measurements: the first had the aim to characterize the new circuits of CITIROC and the second was performed to evaluate the optical cross talk and the gain variation for the SiPM configuration with the logical pixels adopted for the ASTRI SST-2M camera. The gain of the LG chain preamplifier is set to 5 to produce a monotonic response up to 2000 pe and the gain of the HG chain preamplifier is set to 150 allowing an almost linear working range up to ~ 100 pe (see Sect. 5.1). The shaping time constant of the signal is fixed to 37.5 ns, producing a nominal peaking time of ~ 50 ns.

For the CITIROC characterization we used an arbitrary pulse-function generator to create a precise input charge. The shape of the signal has been tailored to the actual shape of the SiPM waveform. It is characterized by a very fast rise time (a few hundreds of ps) followed by an exponential decay (~ 175 ns). The amplitude of this signal is $103 \pm 4 \mu\text{V}$ for an input charge of 0.12 pC, equivalent to 1 pe for a SiPM operating at a gain of 7.5×10^5 .

The second set of measurements uses the setup shown in Fig. 5: the SiPM and the front-end electronics are located in a small metal box which is placed inside a controlled temperature chamber. The gain is finely tuned changing the operating voltage through a DAC in steps of a few millivolt in a range 71.60 - 72V .

For these measurements we used a light pulse, emitted by a blue light emitting diode (B-LED) facing the SiPM pixels driven by the pulse generator.

All measurements presented in this paper were performed using only one of the 32 channels available in the CITIROC.

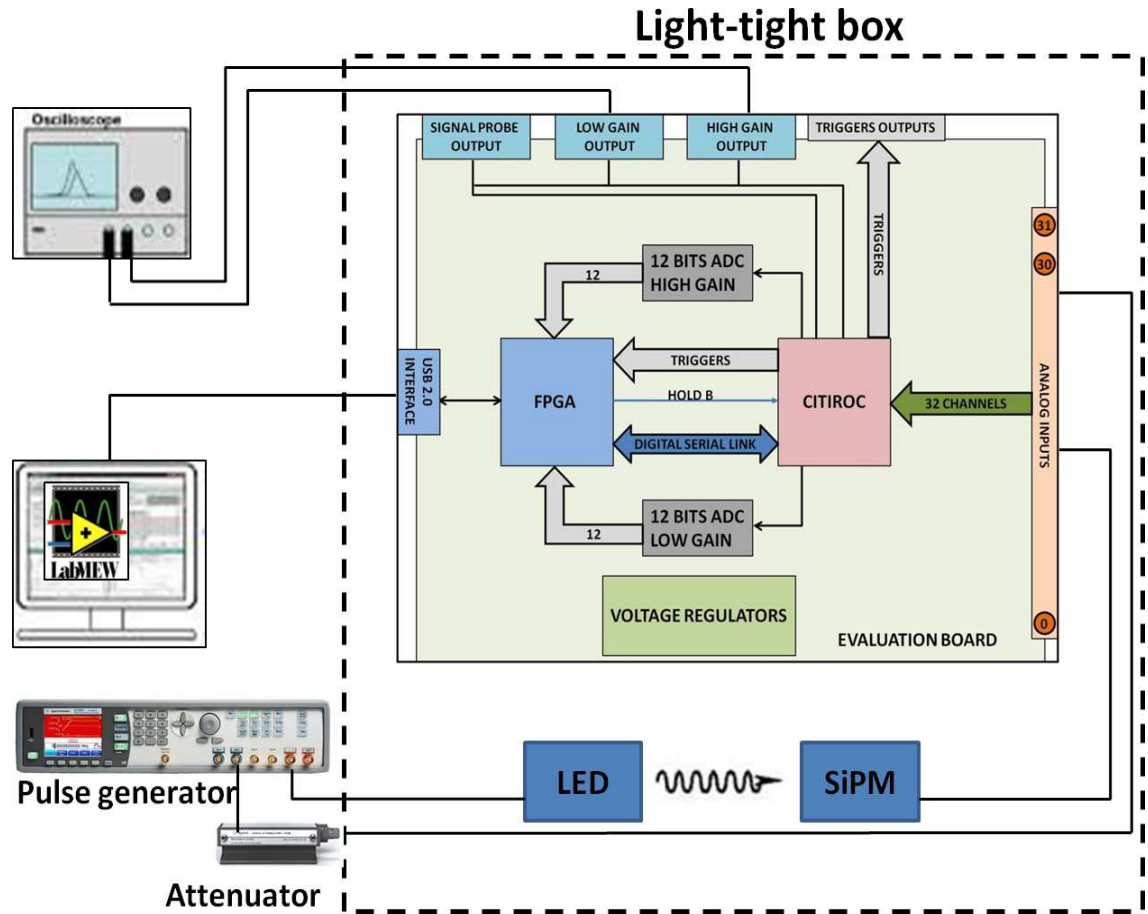


Figure 5: Schematic view of the set-up used for the SiPM+CITIROC characterization.

5. CITIROC characterization

In this set of measurements, we compared the CITIROC energy resolution with that of EASIROC and investigated the response linearity. Moreover, we measured the trigger efficiency as a function of the input charge to complete the characterization published in [14].

5.1. Performance of the Peak detector

5.1.1. Energy resolution

To reduce the degradation of the energy resolution due to incoherent sampling of the signal in EASIROC switched capacitor array (SCA) mode, we introduced also an mode based on the peak detector circuit. As shown in figure 6, this mode, at difference from SCA, keeps the maximum value once it has been reached. To test its performance, we compared the 10 pe pulse-height distributions obtained with CITIROC with those given by EASIROC. The distributions are generated sampling the HG shaped signal from 55 ns to 70 ns in steps of 2 ns with 5000 events per run: results are shown in Fig. 7. Fitting the two curves with Gaussians, we find that the sigma of the peak detector distribution (6.17 ± 0.06) is significantly lower than that of the SCA (9.6 ± 0.1) and is compatible with the intrinsic energy resolution (6.20 ± 0.06) of the SiPM.

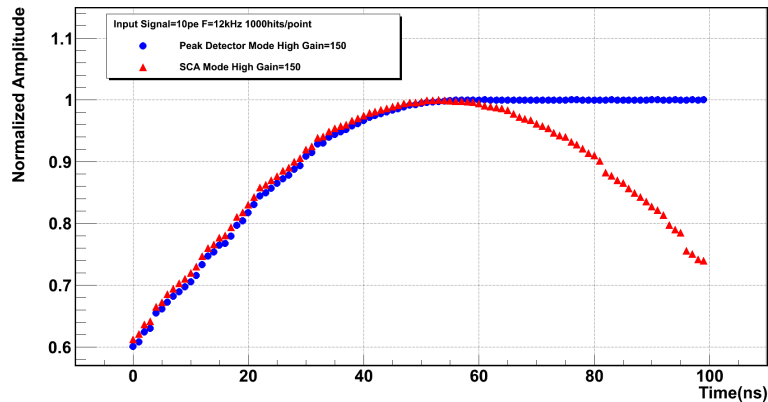


Figure 6: Normalized amplitude of HG shaping function versus time in ns. The red triangles are relative to the SCA mode, and the blue dots show the peak detector mode.

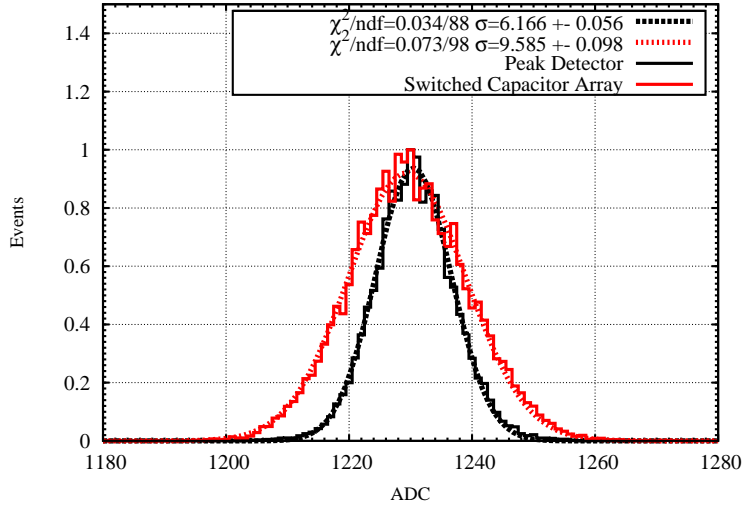


Figure 7: Normalized histograms for injected charge of 10 pe obtained with the peak detector (continuous black line) and the switched capacitor array (continuous red line). The dashed lines represent the fitting functions.

5.1.2. Linearity

We tested the linearity of the response in the HG and LG chains as a function of the input charge by varying it from 0.12 to 15 pC (1-125pe) for the HG and from 6 to 300 pC (50-2500pe) for the LG. For each point, we collected the distributions of the sampled signal over 5000 tests. The ADC values and the errors related to each charge are computed from the average and the sigma of the distributions. Results are shown in Figures 8 and 9. We note that the ADC curves are linear up to 11.4 pC (95 pe) in the HG chain and from 24 pC up to 252 pC (200-2100pe) in the LG chain, with residuals lower than 1%.

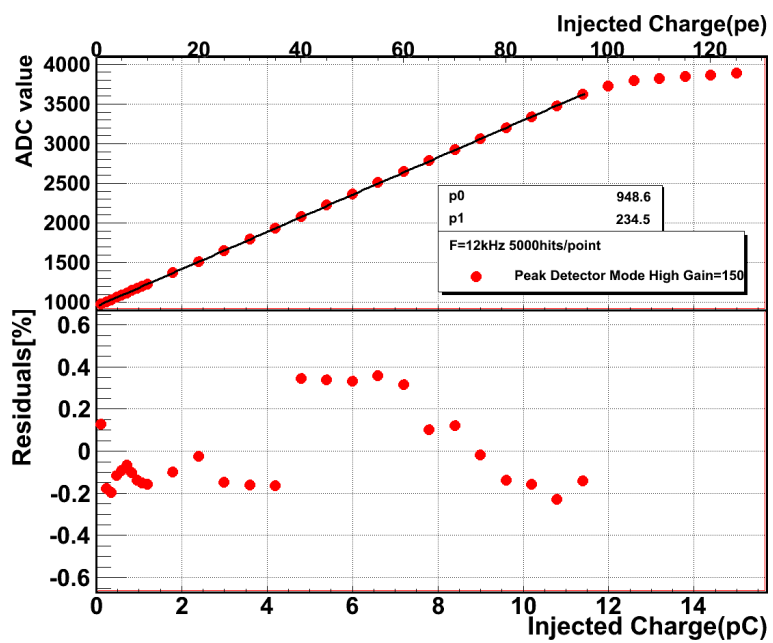


Figure 8: ADC values versus injected charges for the HG chain. The black line is the linear fit up to 95 pe where the ADC value saturates. The p_0 and p_1 are the coefficients of the best fit. The bottom panel shows the residuals respect to the line.

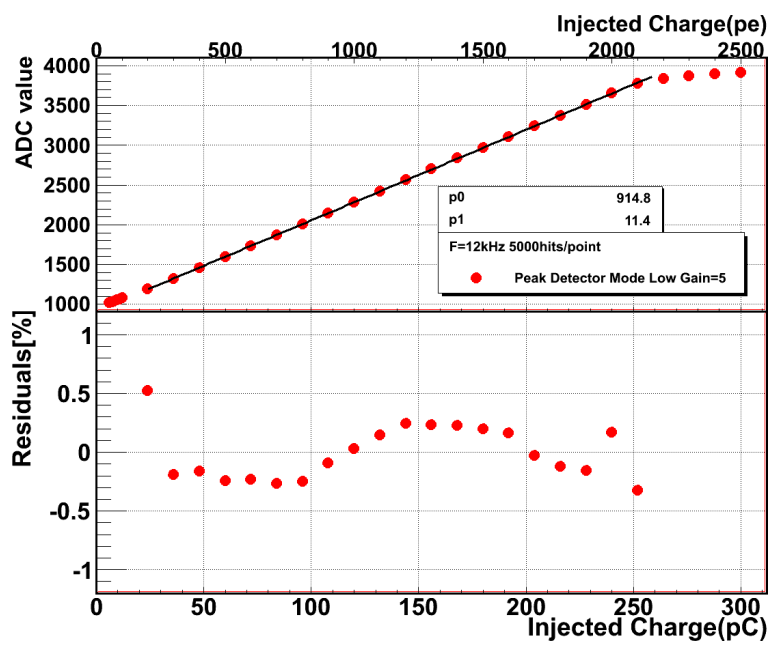


Figure 9: ADC values versus injected charges for the LG chain. The black line is the linear fit in the range 200-2100pe. The p_0 and p_1 are the coefficients of the best fit. The bottom panel shows the residuals respect to the line.

5.2. Trigger linearity and efficiency

To check the linearity of the ASIC discriminator, we studied the curves of the trigger efficiency as a function of threshold. They are obtained by varying the input charge and the threshold level while the other parameters, such as the preamplifier gain and shaping time, are kept constant. Figure 10 shows the evolution of 50% of trigger efficiency as a function of the injected charge in the range 0.12-3.84 pC (1-32 pe). The trigger efficiency is linear, with a discrepancy lower than 1% up to 2.64 pC (22 pe) and it saturates at 32 pe.

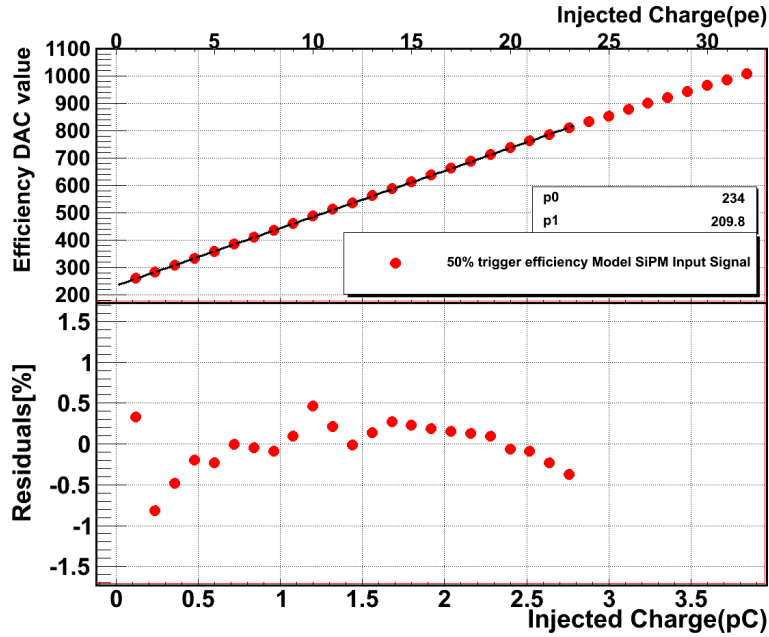


Figure 10: 50% trigger efficiency threshold versus injected charge from 0.12 to 3.84 pC. The p_0 and p_1 are the coefficients of the best fit. The bottom panel shows the residuals respect to the line.

6. Characterization of the SiPM configuration with logical pixel

The SiPM physical pixel ($3 \times 3 \text{ mm}^2$) characterization has been already done and the results have been published in [16]. The measurements presented in

this paper refer to the logical pixels configuration ($6.2 \times 6.2 \text{mm}^2$) adopted for the ASTRI SST-2M camera.

6.1. Optical cross talk

The optical cross talk level was evaluated by measuring the dark count rate as a function of the discriminator threshold. Assuming a Poisson distribution, the probability to have two coincident events within a time window of 15 ns is about 0.001% for the laboratory measured rate of 1 MHz: all events with a number of pe higher than 1 are due to optical cross talk. The dark count rate drops when integer multiples of 1 pe thresholds are reached: the total rate is obtained with thresholds above the electronic noise but below 1 pe; conventionally it refers to 1/2 pe. The characteristic curve obtained varying the discriminator threshold is known as "staircase".

In this set of measurements, we varied the operating voltage in the range 71.60-72.00V in steps of 100 mV, keeping the temperature constant at $15.0^\circ\text{C} \pm 0.1^\circ\text{C}$. We accumulated the staircases for several operating voltages as shown in the top panel of Figure 11. The optical cross talk probability is measured with the ratio between the rate relative to 1 pe (ν_{1pe}) and that corresponding to 2 pe (ν_{2pe}), $P_c = \nu_{2pe}/\nu_{1pe}$, following the method applied in a first evaluation with the front-end EASIROC [17]. The discriminator thresholds to evaluate ν_{1pe} and ν_{2pe} are obtained computing the first derivative of the staircases and evaluating the maxima of the curves by fitting the data with a spline function.

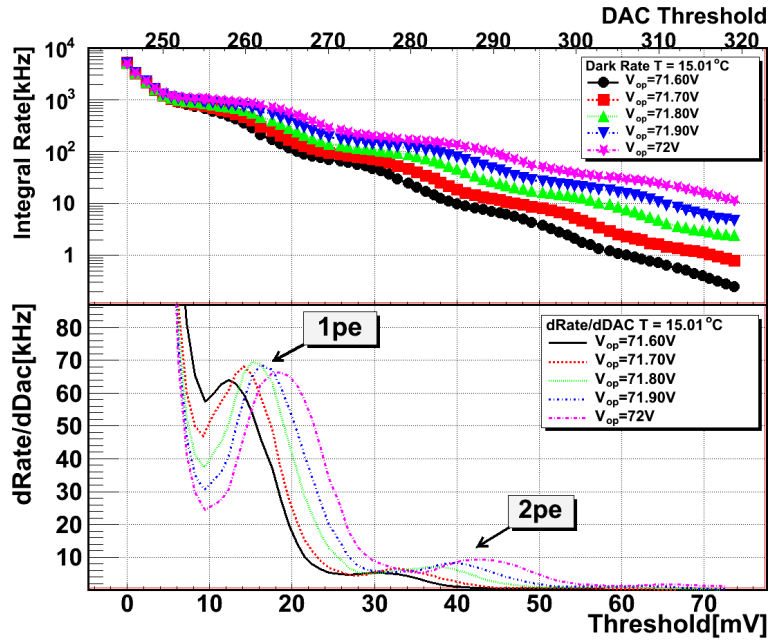


Figure 11: *Top panel:* Dark rate as a function of the discriminator threshold at the fixed temperature of 15.01°C and at different operating voltages values. *Bottom panel:* First derivative of the dark rate vs the discriminator threshold, the arrows indicate the position where ν_{1pe} and ν_{2pe} are computed.

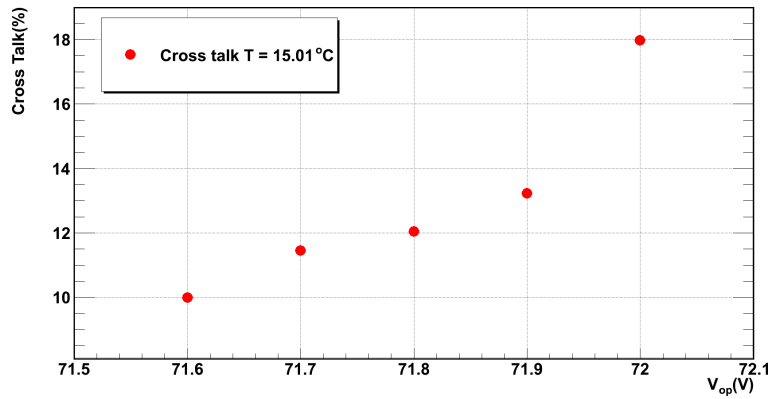


Figure 12: Optical cross talk probability versus operating voltage at 15.01°C . The error of each point is less than 0.1 %, so it is not visible in the figure

As a result, figure 12 presents the optical cross talk values as a function of

the operating voltage: it increases from 10% to 18% in the investigated range. These values are comparable to those measured in the SiPM characterization presented in [16] for the physical pixels.

6.2. Gain variation as function of temperature and voltage

To evaluate the gain, we used the pulse height distribution measured by pulsing a B-LED at a constant rate of 10 kHz. The duration of the B-LED pulse was set in order to have an average number of pe ~ 4 . All results are then obtained for the HG chain. Figure 13 shows the integrated charge spectra at the investigated voltage values accumulated keeping the temperature at 15.01°C. The first peak, referred to as "pedestal", includes events due to electronic noise and SiPM noise. The gain G in each histogram is determined from the average of the ADC distances between subsequent local maxima applying the following equation :

$$G = \frac{1}{N} \cdot \sum_{i=1}^N (ADC_{i+1} - ADC_i) \quad (1)$$

where G is given in ADC units, ADC_i is the ADC value of the maximum of the i -th peak on the histogram while N is the number of peaks. The error on G is given by the standard deviation of the measured value with respect to the mean.

We investigated the variation of the gain with voltage (dG/dV) in the range 71.60-72.00V. Using a linear fit for all the data we obtain the following relation (see figure 14):

$$\frac{dG_{ADC}}{dV} = 14.76 \quad [ADC/V] \quad (2)$$

where the gain is expressed in unit of ADC code.

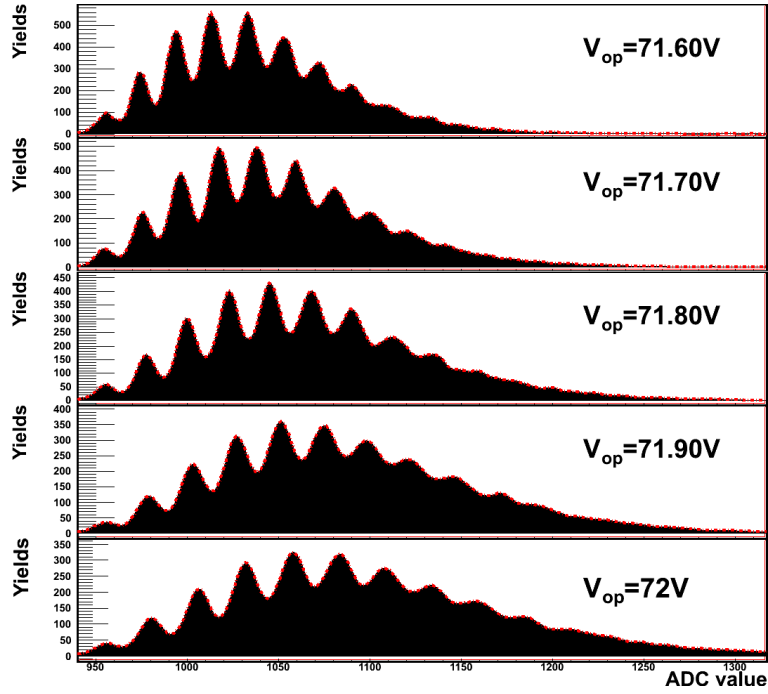


Figure 13: Pulse height distributions for operating voltages in the range (71.60-72.00)V, computed at temperature $T=15.01^{\circ}\text{C}$.

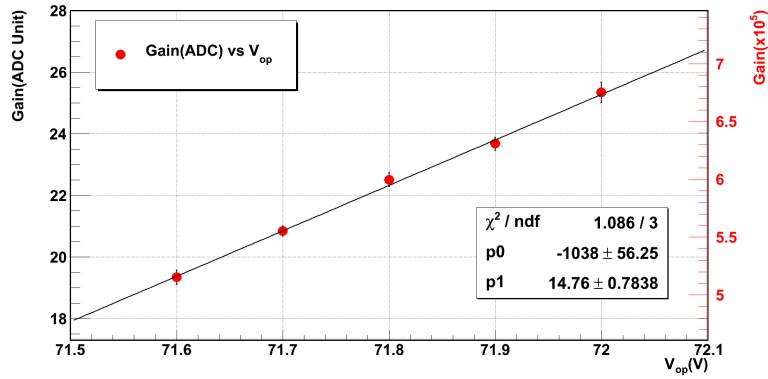


Figure 14: Gain variation in ADC units as a function of the V_{op} at 15.01°C . For clarity, the correspondent absolute value of the gain is reported on the right.

Considering that the electronics does not introduce any variation with temperature, as we tested in laboratory, we also investigated the SiPM gain de-

pendence on the temperature (dG/dT) with the same method described above. Figure 15 shows the resulting pulse height distributions obtained varying the temperature from 13°C to 17°C for a fixed operating voltage of 71.80 V.

The points are well inside a linear relationship as shown in figure 16; the slope is given by the following equation:

$$\frac{dG_{ADC}}{dT} = -1.06 \quad [ADC/^\circ C] \quad (3)$$

where the gain is expressed in unit of ADC code.

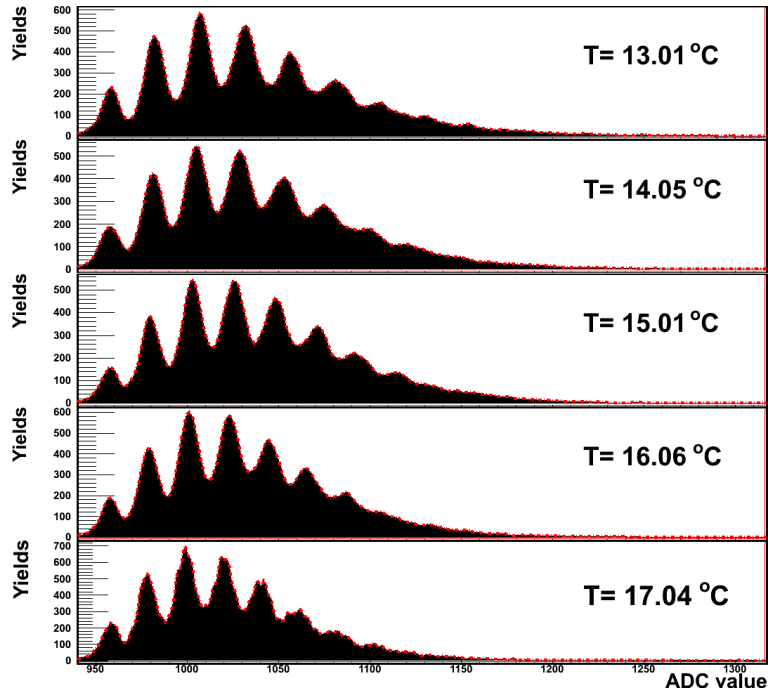


Figure 15: Pulse height distributions for several temperatures at the operating voltage of 71.80 V.

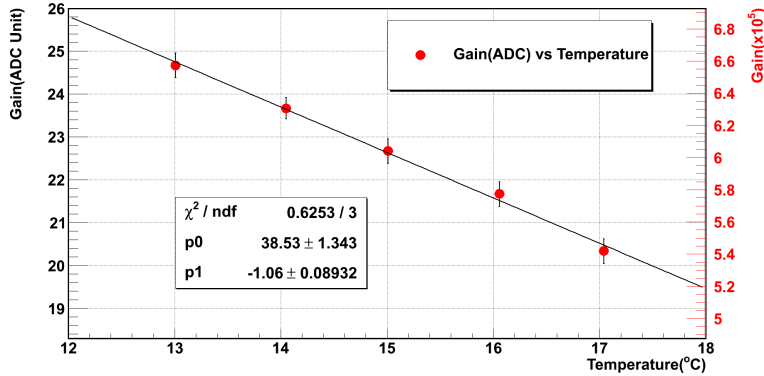


Figure 16: Gain variation in ADC unit as a function of the temperature at 71.80 V. For clarity, the correspondent absolute value of the gain is reported on the right.

7. Conclusions

We presented a set of measurements aimed at characterizing the peak detector circuit implemented in CITIROC. Moreover, we evaluated the level of optical cross talk and the rate of the gain variations as a function of temperature and operating voltage for the SiPMs Hamamatsu S11828-3344m adopted for the ASTRI SST-2M camera. Our results can be summarized in the following points:

- CITIROC overcomes the problems introduced by the SCA mode and allows for coherent sampling of the pixels fired by the shower even in case of large (~ 30 ns) image time gradient. This results in improved energy resolution.
- The signal is linear with respect to the input charge up to 100 pe in HG and up to 2000 pe in the LG. The trigger dynamic range extends linearly up to 17 pe and saturates at 32 pe.
- The SiPM Hamamatsu S11828-3344m adopted for ASTRI SST-2M has an optical cross talk level in the range 10-20%. ASTRI SST-2M will be

operated with SiPM gains resulting in an optical cross talk lower than 15% even if this implies a loss in the linearity for low input charges.

The updated versions of the sensor foreseen for the ASTRI/CTA mini-array are expected to have a level of optical cross talk of a few percent.

- We evaluated the function that models the variation of the gain with respect to voltage and temperature. We find a good linearity in the investigated range: the gain increases by 14.76 ADC per volt, and decreases by 1.06 ADC for an increase of one degree in temperature.

We can conclude that the CITIROC ASIC is fully suitable for ASTRI SST-2M and it can also be adopted in any new version of SiPM that could be proposed for ASTRI/CTA mini-array.

8. Acknowledgements

The work presented in this paper was supported in part by the ASTRI, "Flagship Project" financed by the Italian Ministry of Education, University, and Research (MIUR) and led by the Italian National Institute for Astrophysics (INAF). We also acknowledge partial support from MIUR Bando PRIN 2009 and TeChe.it 2014 Special Grants. We are deeply grateful to S. Callier, C. De La Taille, J. Fleury and L. Raux within WEEROC at Orsay and to the ASTRI collaborators for useful discussions and suggestions. D.I., S.G., T.M. and O.C. thank M. Fiorini, E. Giro, M.C. Maccarone, S. Vercellone and S. Wakley for their contributions as internal referees of the paper.

References

- [1] Acharya, B. S. et al., "Introducing the CTA concept", *Astroparticle Physics* 43, 3 (2013).
- [2] Actis, M. et al., "Design concepts for the Cherenkov Telescope Array CTA: an advanced facility for groundbased high-energy gamma-ray astronomy", *Experimental Astronomy* 32, 193 (2011). arXiv:1008.3703.

- [3] La Palombara, N. et al., for the ASTRI Collaboration, "The INAF ASTRI Project in the framework of CTA", in: Proceedings of the ICATPP-2013 Como, World Scientific, 2014 arXiv:1405.4187.
- [4] Canestrari, R. et al., for the ASTRI Collaboration and the CTA Consortium, "The ASTRI SST-2M prototype: structure and mirror", in: Proceedings 33rd of the ICRC2013, 2-9 July 2013, Rio de Janeiro Brazil, (arXiv:1307.4851).
- [5] Bonnoli, R. et al., for the ASTRI Collaboration and the CTA Consortium, "Boosting the performance of the ASTRI SST-2M prototype: reflective and anti-reflective coatings", in Proceedings 33rd of the ICRC2013, 2-9 July 2013, Rio de Janeiro Brazil, (arXiv:1307.5405).
- [6] Catalano, O. et al., For the ASTRI collaboration, "The ASTRI SST-2M prototype: camera and electronics", in: Proceedings ICRC 2013, Rio De Janeiro, Brazil, July 2013.
- [7] Catalano, O. et al., For the ASTRI Collaboration and the CTA Consortium, "The camera of the ASTRI SST-2M prototype for the Cherenkov telescope array", in: Proceedings SPIE 2014 Ground-Based and Airborne Instrumentation for Astronomy, vol. 91470D, Montreal, Canada, June 2014.
- [8] Billotta, S. et al., for the ASTRI Collaboration and the CTA Consortium, "SiPM detectors for the ASTRI project in the framework of the Cherenkov telescope array", in: Proceedings SPIE 2014 High Energy Optical and Infrared Detectors for Astronomy VI, vol. 91541R, Montreal, Canada, July 2014.
- [9] Bonanno, G. et al., "Characterization Measurements Methodology and Instrumental Set-up Optimization for New SiPM Detectors - Part I: Electrical Tests", IEEE Sensors Journal 14, 10 (October), 2014, 3557.
- [10] Bonanno, G. et al., "Characterization Measurements Methodology and In-

strumental Set-up Optimization for New SiPM Detectors - Part II: Optical Tests”, IEEE Sensors Journal 14, 10 (October), 2014, 3567.

- [11] Marano, D. et al., ”PSPICE High-Level Model and Simulations of the EASIROC Analog Front-End”, International Journal of Modelling and Simulations 34 (4), 2014.
- [12] Callier, S. et al., ”EASIROC, an easy & versatile readout device for SiPM”, TIPP 2011 Technology and Instrumentation in Particle Physics 2011.
- [13] Impiombato, D. et al., on behalf of the ASTRI Collaboration, ”Characterization of the front-end EASIROC for readout of SiPM in the ASTRI camera”, in: Proceedings of the SciNeGHE 2012 Workshop, 20-22 June 2012, Lecce, Italy, (Nuclear Physics B (Proceedings Supplements) 239 (June 2013) 254).
- [14] Impiombato, D. et al., on behalf of the ASTRI Collaboration, ”Characterization of EASIROC as front-end for the readout of the SiPM at the focal plane of the Cherenkov telescope ASTRI” Nuclear Instruments and Methods in Physics Research Section A 729 (November), 2013, 484.
- [15] Fleury, J. et al., ”Petiroc and Citiroc : Front-end ASICs for SiPM readout and ToF applications”, Journal of Instrumentation 9, 2014, C01049.
- [16] Marano, D. et al., ”Electro-optical characterization of MPPC detectors for the ASTRI Cherenkov telescope camera”, Nuclear Instruments and Methods in Physics Research Section A 768, 2014, 32.
- [17] Impiombato, D. et al., on behalf of the ASTRI Collaboration, ”Evaluation of the optical cross talk level in the SiPMs adopted in ASTRI SST-2M Cherenkov Camera using EASIROC front-end electronics” Journal of Instrumentation 9 (02), (article id. C02015).